

ROTATION RATE OF HIGH LATITUDE AND NEAR POLAR CORONAL HOLES

K. M. Hiremath^{1,2}, Manjunath Hegde¹ and K. R. Varsha³

1. Indian Institute of Astrophysics, Bangalore, India, Email: hiremath@iiap.res.in
2. #23, Mathru Pithru Krupa, 2nd Cross, 1st Main, BDA Layout, Bikasipura, BSK V Stage, Bengaluru-560111, India
3. No 204, 2nd Cross, VBHCS, R.R Nagar, Bengaluru - 560098, India

ABSTRACT

For the period of 1997-2006, coronal holes detected in the SOHO/EIT 195 Å full disk calibrated images are used to compute the rotation rates of high latitude and near polar coronal holes and, their latitudinal variation is investigated. We find that, for different latitude zones between 80° north and 75° south, for all their area, the number of days observed on the solar disk, and their latitudes, coronal holes rotate rigidly. Estimated magnitudes of sidereal rotation rate of the coronal holes are: 13.051 ± 0.206 deg/day for the equator, 12.993 ± 0.064 deg/day in the region of higher latitudes and, 12.999 ± 0.329 deg/day near the polar regions. For all the latitudes and the area, we have also investigated the annual variation of rotation rates of these coronal holes. We find that, for all the years, coronal holes rotate rigidly and their magnitude of equatorial, high latitude and polar region rotation rates are independent of magnitude of solar activity.

1 INTRODUCTION

Solar coronal holes (CHs) are observed in EUV and Xray images as dark features, whereas these activity features appear as bright features in the He I 10830 Å (Harvey and Sheeley 1979). Depending upon observed wavelengths, coronal holes either partly or predominantly are associated with the large-scale unipolar magnetic field structure of the sun. CHs are large regions in the solar corona with low density plasma (Krieger *et. al* 1973, Neupert and Pizzo 1974, Nolte *et.al.* 1976, Zirker 1977, Cranmer 2009, Wang 2009). CHs are the source regions of fast solar wind (Altschuler 1972, Temmer *et. al.* 2007, Hegde *et.al.* 2015). Recent studies (Soon *et.al.* 2000, Shugai *et.al.* 2009, Verbanac *et.al.* 2011) show that (Harvey and Sheeley 1979, Krieger *et. al* 1973, Neupert and Pizzo 1974, Nolte *et.al.* 1976, Zirker 1977) on short time scales, occurrences of solar coronal holes trigger responses in the Earth's upper atmosphere and magnetosphere apart from sunspot and magnetic activity (Hiremath 2009 and references there in).

For better understanding of solar activity, idea of rotational structure of different layers i.e, interior, surface and atmosphere of sun are essential. Currently, there is a general consensus regarding the interior rotation as inferred from the helioseismology (Dalsgaard and Schou, Antia *et.al.* 1998, Thompson *et.al* 2003, Howe 2009, Antia and Basu 2010). Also, we have the knowledge of surface rotation rates derived from sunspots (Newton and Nunn 1951, Howard *et.al.* 2084, Balthasar *et.al* 1986, Sivaraman *et.al.* 1993, Javaraiah 2003), Doppler velocity (Howard and Harvey 1970, Ulrich *et.al* 1988, Snodgrass and Ulrich 1990) and magnetic activity features (Wilcox and Howard 1970, Snodgrass 1983, Komm

et.al. 1993). But the magnitude and form of rotation law for features in the corona show different natures (Hiremath and Hegde 2013, and references there in).

Although there is a general consensus regarding surface (derived from the sunspots and Doppler velocity) and internal rotation (inferred from the helioseismology) rate of the sun, whereas right from discovery of coronal holes, there is no consensus regarding rotation rate, whether these coronal activities rotate rigidly or differentially. From the detected coronal holes in different spectral windows, some studies (Shelke and Pande 1985, Obridko and Shelting 1989, Navaro and Sanchez 1994, Insley *et. al.* 1995, Oghrapishvili *et. al.* 2018) show that coronal holes rotate differentially and, other majority of studies came to a conclusion that the coronal holes rotate rigidly (Wagner 1975, Wagner 1976, Timothy *et. al.* 1975, Bohlin 1977, Hiremath and Hegde 2013, Japaridze *et.al.* 2015, Bagashvili *et.al* 2017, Prabhu *et.al* 2018).

Using KPNO helium synoptic charts, rotation rates of equatorial and high latitude coronal holes (Shelke and Pande 1985) are computed and it is found that coronal holes rotate rigidly. For the years 1978-1986, Obridko and Shelting (1989) analyzed the synoptic charts of solar geophysical data and came to the conclusion that coronal holes rotate differentially. From the analysis of of 18 yrs of coronal hole data, Navaro and Sanchez (1994) came to the following conclusions: (i) for all latitude, coronal holes rotate differentially, (ii) below 40 deg latitude, magnitude of rotation rate of coronal holes increases towards the equator, (iii) whereas, rotation rate of coronal holes above 40 deg latitude increases towards pole. From the analysis of He 10830 Å coronal hole data, Iinsle *et. al.* (1995) found that coronal holes rotate differentially. Very recently, Oghrapishvili (2018) used two years SDO/AIA data of coronal holes and similar to previous studies, these authors also came to a conclusion that coronal holes rotate differentially.

Pioneering studies (Wagner 1975, Wagne 1976) on the rotation rate of the coronal holes that are analyzed from the Fe XV (284 Å) data showed that coronal holes rotate rigidly. The coronal holes observed in the same wave length were used by Timothy *et. al.* (1975) and obtained the result that coronal holes rotate rigidly. From the evolutionary and rotational characteristics, these authors conclude that coronal holes probably might have originated below the photosphere. Continuing with the same coronal hole data, Bohlin (1977) also came to a similar conclusion of rigid body rotation rate of the coronal holes. For the years 2001-2008 and from the full-disk SOHO/EIT 195 Å near equatorial coronal hole data, Hiremath and Hegde (2013) showed that irrespective their area and latitude, coronal holes rotate rigidly. Further, from the area evolutionary and dynamical characteristics, with reasonable theoretical arguments, Hiremath and Hegde (2013) showed that coronal holes probably might be originated below base of the convection zone. From the Kitt Peak Observatory He I 10830 Å coronal hole data and for the years 2003-2012, Japaridze *et.al.* 2015 showed that coronal holes have magnitude of rotation rate of 13.39 deg/day and rotate rigidly compared to photospheric tracer rotation rates. Bagashvili *et.al* (2017) analyzed SDO/AIA 193 Å coronal hole data and two important results relevant to the present study are: (i) coronal holes rotate rigidly and, (ii) coronal hole rotation rate latitudinal profile perfectly matches only with the latitudinal rotational rate of the solar plasma around $0.71 R_{\odot}$, near lower layers of base of convection zone. Very recent study (Prabhu *et.al* 2018) that used the recurrent coronal hole data of He 10830 Å and

EUV 195 Å came to the conclusion that coronal holes rotate rigidly and conjectured that these coronal hole activity features might have originated below base of convection zone.

Most probable reasons for these contradicting results on rotation rate of the coronal holes are the following: (i) lack of correct methods for detection of coronal holes, especially during the initial period of discovery of coronal holes, and their accurate determination of heliographic coordinates and, (ii) not taking into account the projectional effects, especially near higher latitudes and near the limbs, for the position of coronal holes. Infact, we have fulfilled these two demands reasonably and accurately in the present study. It is also to be noted that most of the afore mentioned studies restricted with in the latitudes of 60 deg north to 60 deg south. However, it is interesting to know whether coronal holes near the polar regions rotate rigidly or differentially.

In addition, there are also following two studies which conclude that, in the lower latitudes, coronal holes rotate differentially whereas in the higher latitudes these features rotate rigidly. Based on the Catalog of Coronal Holes, Navaro and Sanchez (1994) found that isolated or equatorial CHs show differential rotation rate while the polar CHs exhibit rigid body rotation rate. Zurbuchen *et.al.* (1996) using SWICS/Ulysses data found that, in the near equatorial and intermediate latitudes, a quasi-rigid rotation rate and no persistent structures at latitudes $>65^\circ$ to determine the polar rotation rate. In continuation of our previous study (Hiremath and Hegde 2013), in the present study, we extend the investigation of rotation rates of coronal holes from near equator to higher latitudes and near polar regions. Although definitions are ad-hoc, according to our definition, equatorial coronal holes are confined to +45 to -45 deg, the higher latitude coronal holes occur in the region of 46 to 65 deg northern and southern hemispheres and, the near polar coronal holes originate in the latitude belt of 66-90 deg in northern and southern hemispheres.

Compared to our previous study (Hiremath and Hegde 2013), this study is different on the four important aspects: (i) in addition to near equatorial coronal holes, in the present study, high latitude and near polar coronal hole rotation rates are also estimated, (ii) in the previous study, we used to detect manually the coronal holes, either ellipse or circle is fitted to the coronal hole and average heliographic coordinates and the area are used to be estimated. However, in the present study, from the morphological image analysis, coronal hole boundary is detected automatically and, average heliographic coordinates and the areas are estimated consistently without any bias, (iii) in the previous study, correct formula for estimation of projectional effects of coronal holes is not used, whereas in the present study correct formula is used, (iv) in the present study, yearly change in rotation rate of coronal holes is investigated, whereas in the previous study it is not.

Using photospheric sunspot and other activity features, there are many studies that deal with the variation of rotation rate of the sun with respect to solar cycle activity. In the present study we also examine variation of rotation rate of coronal holes and different coefficients of law of rotation rates with respect to activity of the solar cycle. Although it appears to be of similar results for all the latitudes, question remains from the previous study that whether coronal holes (at the high-latitude and near polar regions) rotate rigidly or differentially; even if it is either rigid or differential body rotation, it is interesting to know sign of third coefficient in the of rotation law (obtained from the least-square fit) is positive or negative (please to be noted that, according to Snodgrass, sign of the third

coefficient is negative, whereas interestingly for the coronal holes it is positive, at present we don't know why this sign is positive).

In section 2, we present the data used and method of analysis, and results of that analysis in section 3. While section 4 ends with the conclusions of the present study.

2 DATA AND ANALYSIS

From 1997-2006, we use full-disk SOHO/EIT images (Delaboudiniere 1995) that have a resolution of 2.6 arc sec per pixel in a band pass around 195 \AA to detect CHs. It is to be noted that there are data gaps in SOHO for June-October 1998 and January-February 1999. The obtained images are in FITS format and the individual pixels are in units of data number (DN). DN is defined as the output of the instrument electronics that corresponds to the incident photon signal converted into charge within each CCD pixel (Madjarska and Wiegmann 2009).

Using the SolarSoft `eit_prep` routine (Freeland and Handy 1998), images are background subtracted, flat-fielded, degrided, and are normalized. Occurrence dates and position of CH are obtained from the “*spaceweather.com*” web site. By using the approximate positions (heliographic coordinates) of CHs from the “*spaceweather.com*” web site, coronal hole region from the SOHO/EIT images are separated for further analysis. We use intensity thresholding technique to identify coronal holes in the images. Krista and Gallagher (2009) pointed out that in case of coronal hole the intensity histogram shows a bimodal distribution (see the middle illustration of intensity histogram in both the upper and lower panels of Fig 1) and the local minimum corresponds to CH boundary threshold. Following this important fact and for each daily image we find this local intensity minimum that is used as a threshold to detect coronal holes in all the latitudes. So, regardless of the phases of solar cycle this method works very well for all the images.

From the basic morphological image processing operations like erosion and dilation, boundary of the coronal holes are detected. With the SolarSoft, individual pixel information (heliographic coordinates such as latitude and longitude and, the DN counts/intensity) enclosing the coronal holes is obtained. Following our previous study (Hiremath and Hegde 2013, equation 1), average heliographic coordinates weighted with intensity (DN counts) is obtained. As each pixel is weighted with intensity, a reasonable average of these two important parameters can be obtained. With this method, errors in the average coordinates can also be obtained. In this way accuracy of these two coordinates can also be estimated.

We followed the following criteria in selecting CHs data. (1) the CH must be compact, independent, and is not elongated, for example, from pole to the equator in latitude, and (2) in order to maintain the original identity, consider only CHs that do not merge with other CHs during their passage. Although this data consists of both low and high latitude data, as for high latitude coronal holes, for each pixel of the detected coronal hole, following corrections for the projectional effects are applied for intensity I (DN counts)

$$I = \frac{I_{obs}}{\cos\delta}, \quad (1)$$

where, I_{obs} is the observed intensity of the coronal hole, $\cos\delta = (\sin B_0 \sin\theta + \cos B_0 \cos\theta \cos l)$, θ and l are heliographic latitude and heliographic longitude from the central meridian of the CH respectively. This projectional ($\cos\delta$ term in the denominator of eqn 1) correction for the intensity of pixel takes into account high latitude and extreme longitude (from the central meridian) coronal holes. Whereas B_0 is the heliographic latitude of the center of the solar disk at the time of observation. After applying correction for projectional effects and following Hiremath and Hegde (2013) (section 2, eqn 1), average heliographic latitude and longitude from the central meridian of the coronal hole are estimated.

Following the previous method (Hiremath 2002) of computation of rotation rates of sunspots, daily sidereal rotation rates Ω_j of the CH are computed as follows

$$\Omega_j = \frac{(L_{j+1} - L_j)}{(t_{j+1} - t_j)} + \delta\Omega, \quad (2)$$

where L_j , L_{j+1} are average longitude from the central meridian of the CH for the two consecutive days t_j and t_{j+1} respectively, $j = 1, 2, ..n-1$, n is number of days of appearance of CH on the visible solar disk and, $\delta\Omega$ is a correction factor for the orbital motion of the Earth around the sun. Strictly speaking, this correction factor is due to orbital motion of the SOHO spacecraft around the sun. Compared to the distance between the sun and Earth, the distance between the SOHO satellite and the Earth is very small and hence orbital distances of Earth and the satellite are almost same and hence the correction factor $\delta\Omega$ is ~ 1 deg/day in order to get the sidereal rotation rate of the coronal holes. For the present work, this approximation is sufficient. However, if one wants to find the long term (greater than 11 yrs) variation of rotation rates, correction factor $\delta\Omega$ should be computed accurately (Roša *et.al.* 1995, Wittmann 1996, Skokic *et.al.* 2014).

3 RESULTS

For the period of observations from 1997 to 2006, a total of 163 CHs satisfy the criteria as given in the previous section. For different years such occurrence number of coronal holes is presented in Fig 2 (a). During their evolutionary passage over the solar disk, we compute rotation rates and assign respective latitudes. In the present study, we consider only non-recurrent CHs that appear and disappear on same part of the visible disk. If such a non-recurrent CH exists for n days, then its life span τ is n days and the total number of rotation rates is $(n - 1)$. Irrespective of their area, in both the hemispheres, rotation rates of coronal holes for each 5° bin are collected and, average rotation rate and its standard deviation are computed. For example, Fig 2(b) illustrates the idea of number of rotation rates in each bin considered for computation of average rotation rate.

3.1 Latitudinal variation of coronal holes

With the constraints of 65 deg east to 65 west of longitude from central meridian and for latitude zone of +45 deg to -45 deg, Figure 3(a) illustrates the latitudinal variation of rotation rate of coronal holes. In this and subsequent Figures, units of rotation rate in the left hand side of y axis is deg/day and on the right hand side of y axis is nHz (in order to compare with the rotation rate of sun's interior inferred by the helioseismology which use nHz as the unit).

With a similar constraint of latitude (65 deg east to 65 west) zone, for the same SOHO/EIT 195 Å and for the years 2001-2008, in the previous study (Hiremath and Hegde 2013, Fig 4(a)) we have obtained the rotation rate profile that yields coronal holes rotate differentially. In fact, it is to be noted that, in terms of magnitude (of both the coefficients), differential rotation rate profile obtained in the present study is almost similar to the rotation rate profile as obtained by our previous study. Whereas, for the same constraint on longitudes, Fig 3(b) illustrates the variation of rotation rate of the coronal holes for latitude zone that varies from 80 deg north to 75 deg south. That means the results presented in both the Figures 3(a) and 3(b) suggest that for all the latitudes coronal holes rotate differentially. In the following, let us examine further whether this picture changes in case we constrain further in longitudes and after taking into account the projectional effects.

For the same constraint of latitude zone, albeit with a constraint of 45 deg east to 45 west longitude zone (from the central meridian), Figures 4(a) and 4(b) illustrate the latitudinal variation of rotation rate of the coronal holes. However, in addition to mentioned constraints, in case of Fig 4(b), projectional effect is also taken into account. Note that when we apply correct constraints, picture of differential rotation rate of the coronal holes changes to rigid body rotation rate. Infact, this conclusion can also be judged from the consistent decrease of magnitude of second coefficient (that represents differential rotation of the mid-latitudes) of law obtained from the least square fit and also decrease in the value of χ^2 (a measure of goodness of fit). Of course one can also argue that the law of fit is up to $\sin^2\theta$ which may not correctly represents the data of high latitude and near polar region coronal holes, for which law of fit should be up to $\sin^4\theta$. In the following, law of fit up to $\sin^4\theta$ is used and examined whether coronal holes rotate differentially or rigidly.

For the constraint of 65 deg east to 65 deg west of longitude from the central meridian, Fig 5(a) illustrates the latitudinal variation of rotation rate of coronal holes whose profile is fitted with a law up to $\sin^4\theta$. Whereas, with the constraint of 45 deg east to 45 deg west of longitudes, Fig 5(b) illustrates the variation of rotation rate of coronal holes whose profile is also fitted with the rotational law up to $\sin^4\theta$. Although both the results illustrated in Fig 5(a) and Fig 5(b) appear that coronal holes rotate differentially, when we apply the projectional corrections, the results unambiguously suggest that (as illustrated in Fig 6) for all the latitudes coronal holes rotate rigidly.

If we compare the coefficients (the law over plotted on Fig 6) of $\sin^4\theta$ obtained by the least square fit with the coefficients of $\sin^4\theta$ obtained by other study (Snodgrass 1983 and references there in) which uses high latitude magnetic activity features and surface plasma rota-

tion (by Doppler shift) as tracers, obviously for all the latitudes coronal holes rotate rigidly. For further clarity of this statement, let us compare both the laws. Snodgrass laws for both the tracers yield: magnetic tracers: $\Omega(\theta) = (14.3065 - 1.9801\sin^2\theta - 2.1485\sin^4\theta) \text{ deg/day}$; Doppler velocity: $\Omega(\theta) = (14.1432 - 1.8132\sin^2\theta - 2.4925\sin^4\theta) \text{ deg/day}$. When we compare Snodgrass surface rotation rate laws with the rotation rate law ($\Omega(\theta) = 13.051 - 0.161\sin^2\theta + 0.111\sin^4\theta$) obtained from coronal holes, following are the notable differences: (i) magnitude of first coefficient is lesser by $\sim 7.2\%$ compared to magnitude of first coefficient of Snodgrass laws, (ii) second and third coefficients are nearly 10% of the second and third coefficients in the Snodgrass laws and, (iii) there is a change in sign (positive) for the coefficient of $\sin^4\theta$ compared to the sign (negative) of coefficient of $\sin^4\theta$ in case of Snodgrass laws. Hence, overall conclusion of this subsection is that, *for all the area and latitude, coronal holes rotate rigidly.*

Another interesting aspect of this study is that, if we consider the first coefficient of rotation law (see Fig 6), irrespective of all the latitudes, coronal holes rotate with a magnitude of ~ 420 nHz. Infact, previous studies (Hiremath and Hegde 2013, Japaridze *et.al.* 2015, Bagashvili *et.al.* 2017, Prabhu *et.al.* 2018) came to a conclusion that anchoring depth of coronal holes is probably below base the convection zone. If we consider magnitude of average rotation rate of coronal hole which is estimated to be ~ 420 nHz, this can be matched only with the rotation rate of the deep interior of radiative core (Antia *et.al.* 1998, Antia and Basu 2010). However, at present, it is not clear how such gigantic coronal holes form in the deep interior and then protrude into the solar atmosphere, corona and beyond. As the genesis of coronal holes is beyond the scope of this study, further theoretical studies and helioseismic inferences are required to prove or disprove the proposition that coronal holes originate in the deep interior.

3.2 Yearly variation of rotation rate of the coronal holes

Many studies show that equatorial and mid-latitude rotation rates derived from sunspots and other activity features of the photosphere vary with the activity of the solar cycle. It is also interesting to examine whether, for all the latitudes considered in this study, rotation rate of the coronal holes remain constant or varies with the solar activity cycle. This study is not the first investigation. By analyzing full disk spectroheliograms in HeI 10830 Å, (Harvey and Sheeley 1987) found that coronal holes rotate more rigidly during the low sunspot activity and there is a substantial variation of rigidity during other periods of the solar activity. For the years 1978-1986, by analyzing solar geophysical coronal hole data, Obridko and Shelting (1989) came to a conclusion that 2-3 yrs before the solar maximum, coronal holes rotate rigidly, whereas during rest of years of solar cycle, coronal holes rotate differentially. Navarro and Sanchez (1994) showed that coronal holes rotate slower during maximum and vice verse during the minimum of the solar activity.

For different years, Figures 7-10 illustrate the latitudinal variation of rotation rates of the coronal holes. As for the gaps in the data during June-October 1998 and January-February 1999, we have considered 7 months (Jan-May, Nov-Dec) data while computing the average rotation rates and 10 months (March-Dec) data during 1999. In all the Figures 7-10, left panel represents the latitudinal variation of rotation rate which is fitted with a

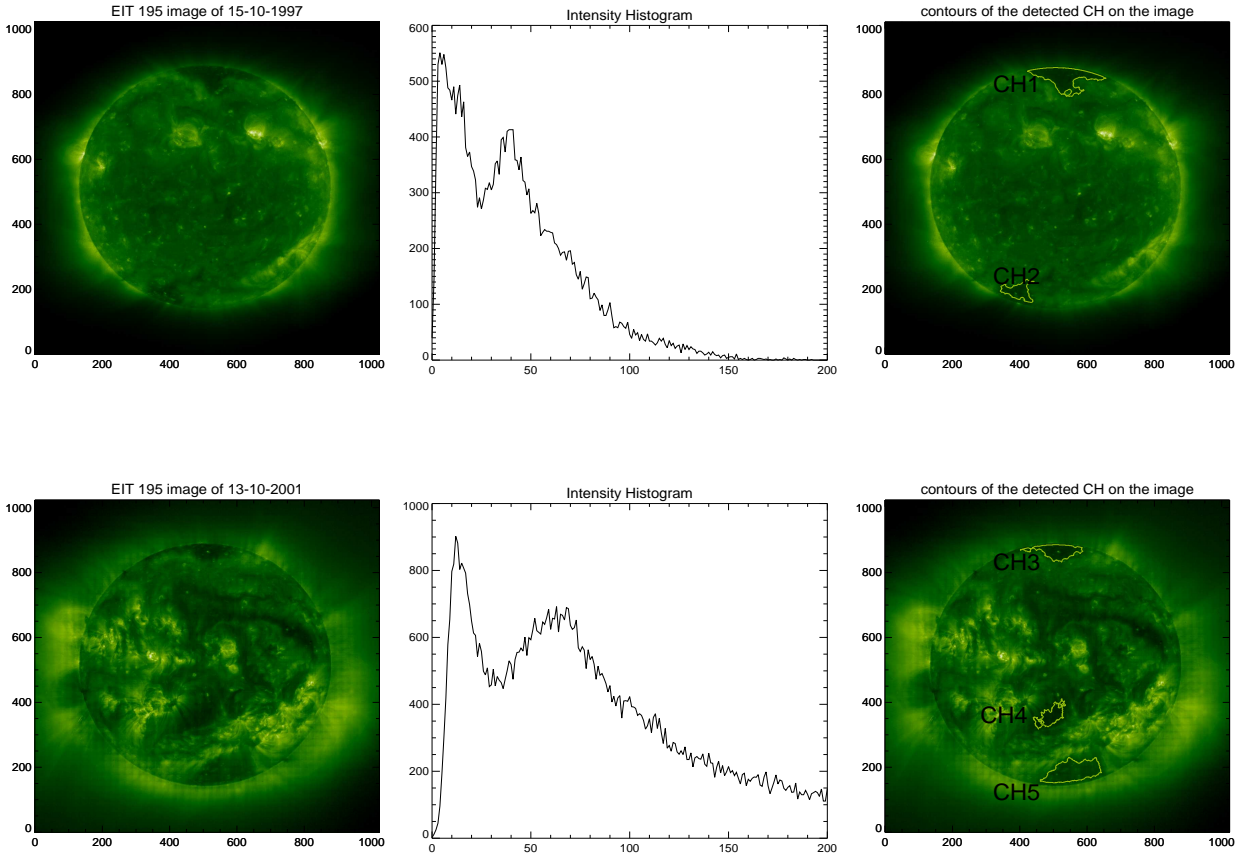


Figure 1: For the observed date 15-10-1997, three successive figures in upper panel represent: SOHO/MDI full disk image observed in 195 \AA , intensity histogram of the full disk image and the detected coronal holes with isocontours as boundary. Whereas lower panel represents for the date 13-10-2001. In both the panels of images CH1 (latitude 75.03 deg North), CH2 (69.94 deg South), CH3 (76.85 deg South), CH4 (20.59 South) and CH5 (61.05 South) are the detected coronal holes respectively.

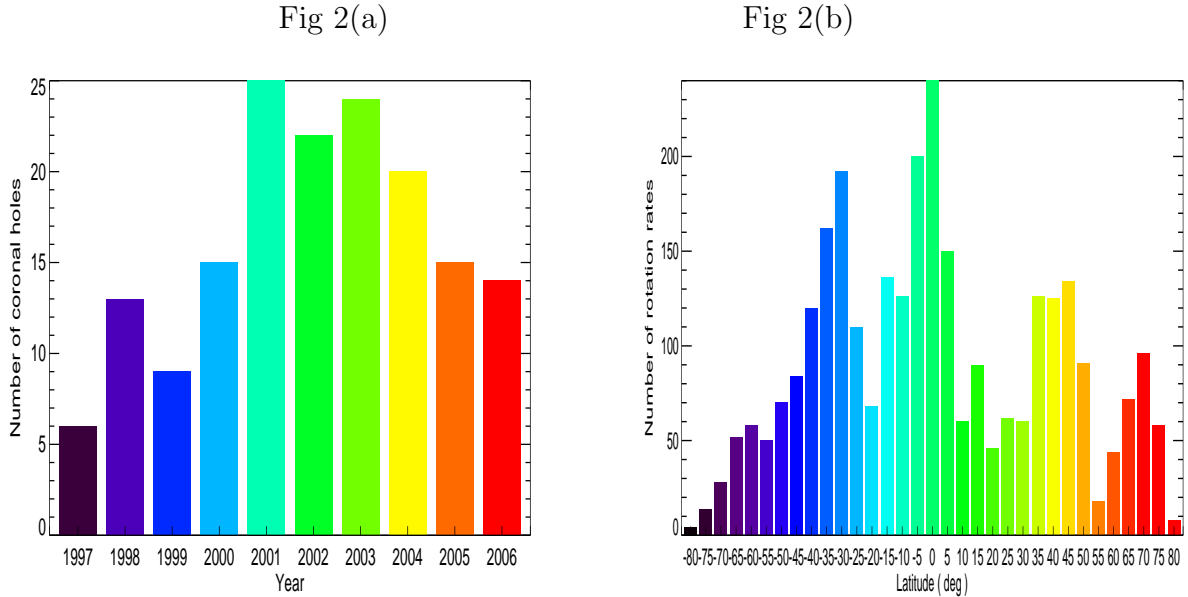


Figure 2: For different years, Fig 2(a) illustrates occurrence number of coronal holes. Whereas Fig 2(b) illustrates the number of rotation rates used for estimation of average rotation rate of the coronal hole in a particular bin.

law up to $\sin^2\theta$ and, right panel is fitted with a law up to $\sin^4\theta$. One can notice from all the Figures 7-10 that, on average, for all the latitudes, rotation rate of the coronal holes is independent of solar activity. Figures 11(a) and 11(b) illustrate the yearly variation of coefficients C_0 and C_1 obtained from the least square fit with a law up to $\sin^4\theta$. Whereas Fig 12 illustrates the annual variation of coefficient C_2 . In all the Figures, although error bars appear to be large, all the three coefficients C_0 (that represents equatorial rotation rate), C_1 (that represents rotation rate of the mid-latitudes) and C_2 (that represents higher latitudes and near polar regions) of least square fit with a law up to $\sin^4\theta$ remain almost constant. Ultimately, from all these results, *it is inevitable to agree that, for all the years and for all the latitudes, rotation rate of the coronal holes is independent of solar activity.* Probably main reason for this yearly constancy of rotation rate of coronal holes, which is different than the previous studies, is that projectional effects for both the higher latitudes and longitudes (from the central meridian) are taken into account in this study, whereas majority of previous studies neglected the same.

4 CONCLUSIONS

For the years 1997-2006, SOHO UV 195 Å data is considered, coronal holes are detected, their average heliographic coordinates such as latitude and longitudes are reasonably and accurately are estimated. After taking into account the projectional effects for both latitude and longitudes, rotation rates of the coronal holes are estimated. It is found that, for all the areas and irrespective of latitude, coronal holes rotate rigidly. Magnitudes of

Fig 3(a)

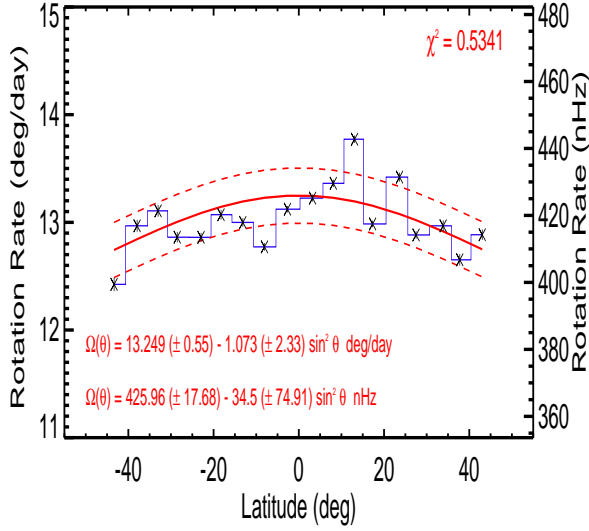


Fig 3(b)

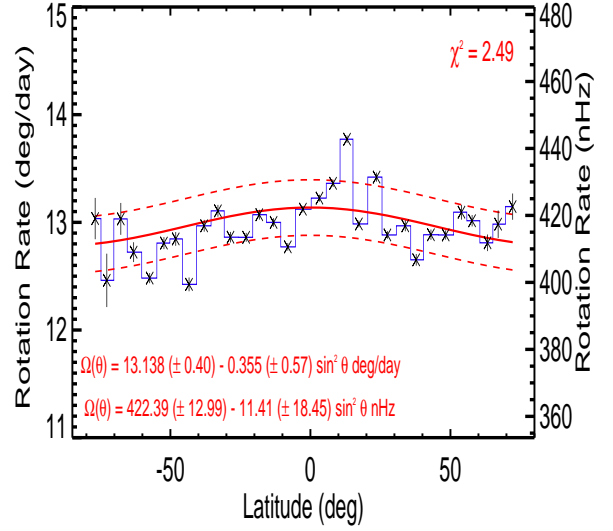


Figure 3: Both the Figures illustrate the variation of rotation rates of coronal holes for the longitude zones 65° east to 65° west from the central meridian. Fig 3(a) for the latitude zones between 45° north to 45° south, whereas Fig 3(b) for the latitude zones from 80° north to 75° south. In both the Figures blue bar curve represents the observed rotation rates; red dashed lines represent the one standard deviation (that is computed from all the data points) error bands and, the red continuous line represents a least-square fit of the observed data with a law of the form $\Omega(\theta) = \Omega_0 + \Omega_1 \sin^2(\theta)$. The χ^2 is a measure of goodness of fit over plotted on both the plots.

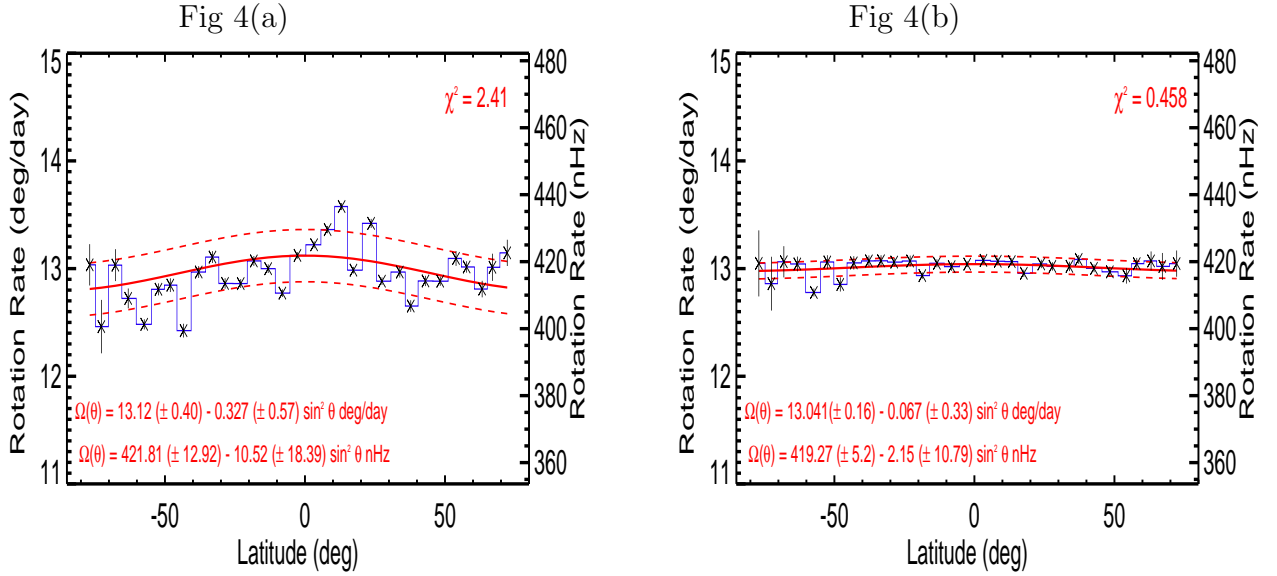


Figure 4: For the longitude zones 45° east to 45° west from the central meridian, both the Figures illustrate the variation of rotation rate of coronal holes with respect to latitudes. In case of Fig 4(b), projectional correction is applied. In both the Figures blue bar curve represents the observed rotation rates; red dashed lines represent the one standard deviation (that is computed from all the data points) error bands and, the red continuous line represents a least-square fit of the observed data with a law of the form $\Omega(\theta) = \Omega_0 + \Omega_1 \sin^2(\theta)$. The χ^2 is a measure of goodness of fit over plotted on both the plots.

Fig 5(a)

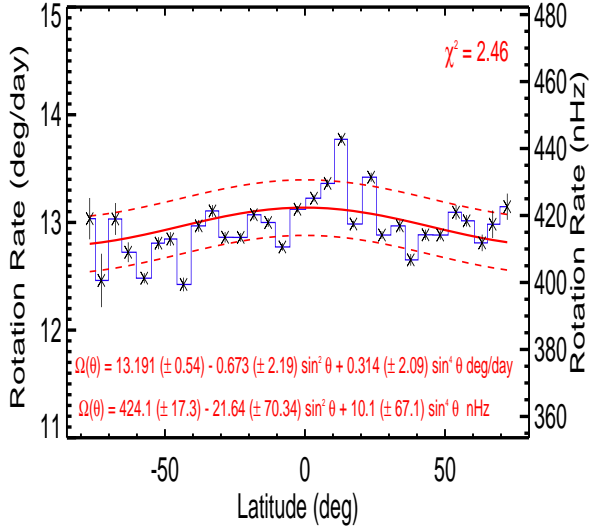


Fig 5(b)

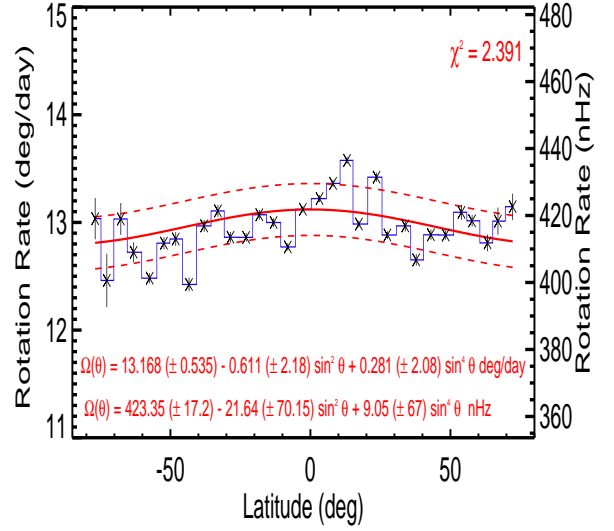


Figure 5: For the longitude zones 65° east to 65° west from the central meridian, Fig 5(a) illustrates the variation of rotation rate of coronal holes with respect to latitudes. Except constraint of 45° east to 45° west from the central meridian, whereas Fig 5(b) represents variation of rotation rate of coronal holes. In both the Figures blue bar curve represents the observed rotation rates; red dashed lines represent the one standard deviation (that is computed from all the data points) error bands and, the red continuous line represents a least-square fit of the observed data with a law of the form $\Omega(\theta) = \Omega_0 + \Omega_1 \sin^2(\theta) + \Omega_2 \sin^4(\theta)$. The χ^2 is a measure of goodness of fit over plotted on both the plots.

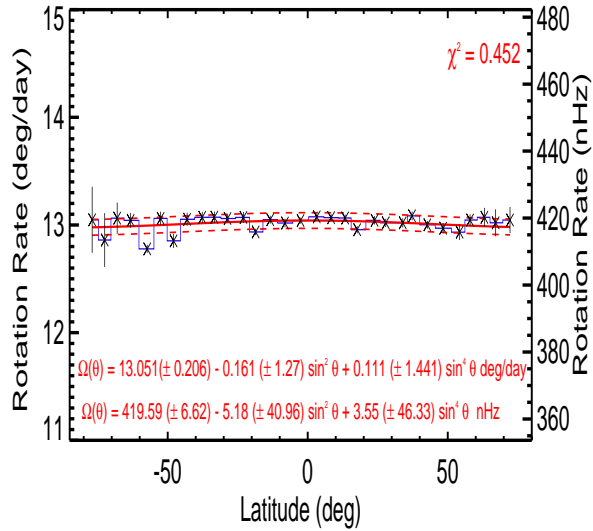


Figure 6: For the same constraints of heliographic latitude and longitudes as presented in Fig 5 and after taking into account the projectional effects, this Figure illustrates the variation of rotation rate of coronal holes with respect to latitudes. Blue bar curve represents the observed rotation rate; red dashed lines represent the one standard deviation (that is computed from all the data points) error bands and, the red continuous line represents a least-square fit of the form $\Omega(\theta) = \Omega_0 + \Omega_1 \sin^2(\theta) + \Omega_2 \sin^4(\theta)$. The χ^2 is a measure of goodness of fit.

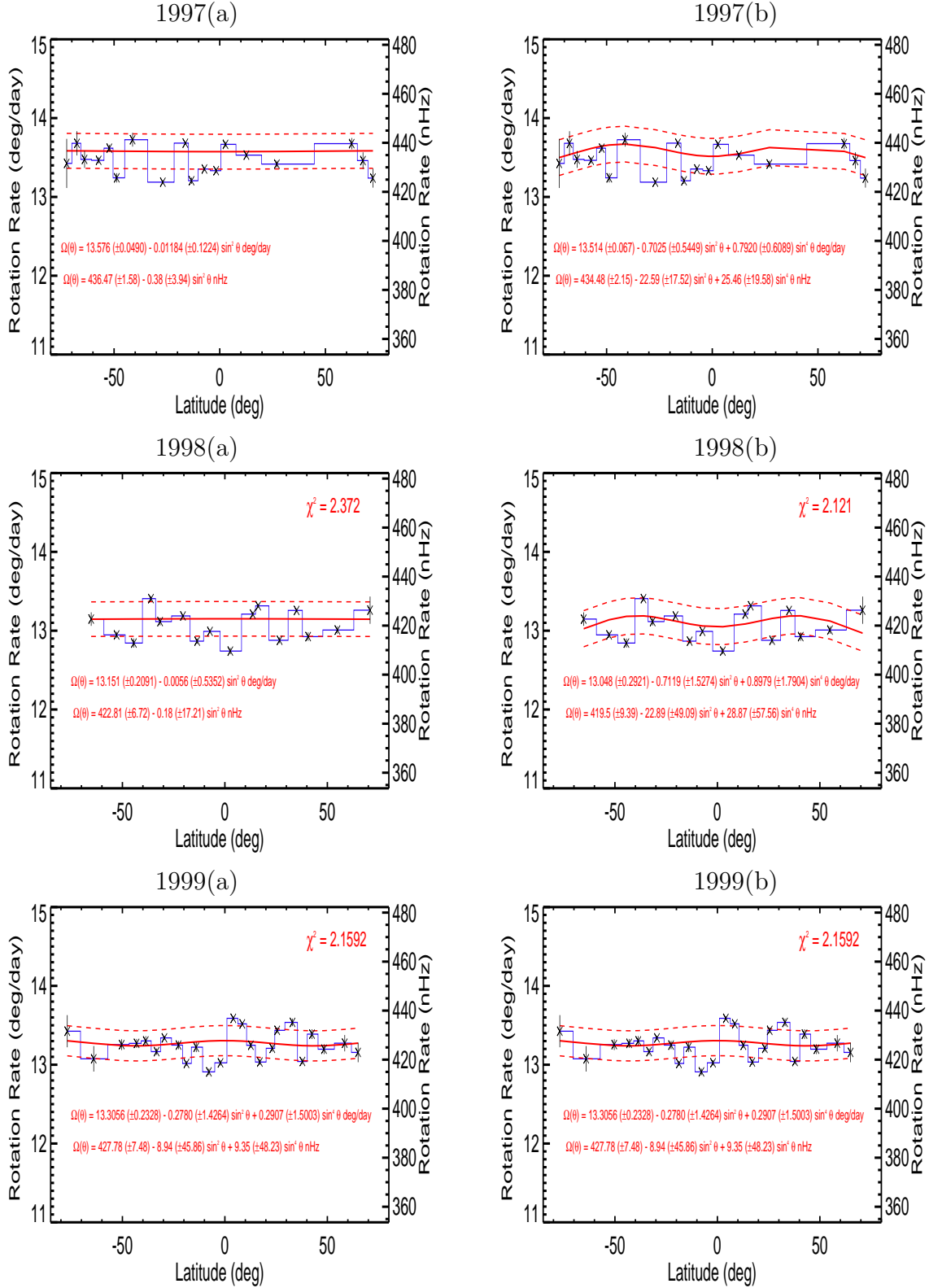


Figure 7: For the years 1997-1999, latitudinal variation of rotation rate of the coronal holes. Left panel is fitted with a law up to $\sin^2\theta$, whereas right panel is fitted with a law up to $\sin^4\theta$.

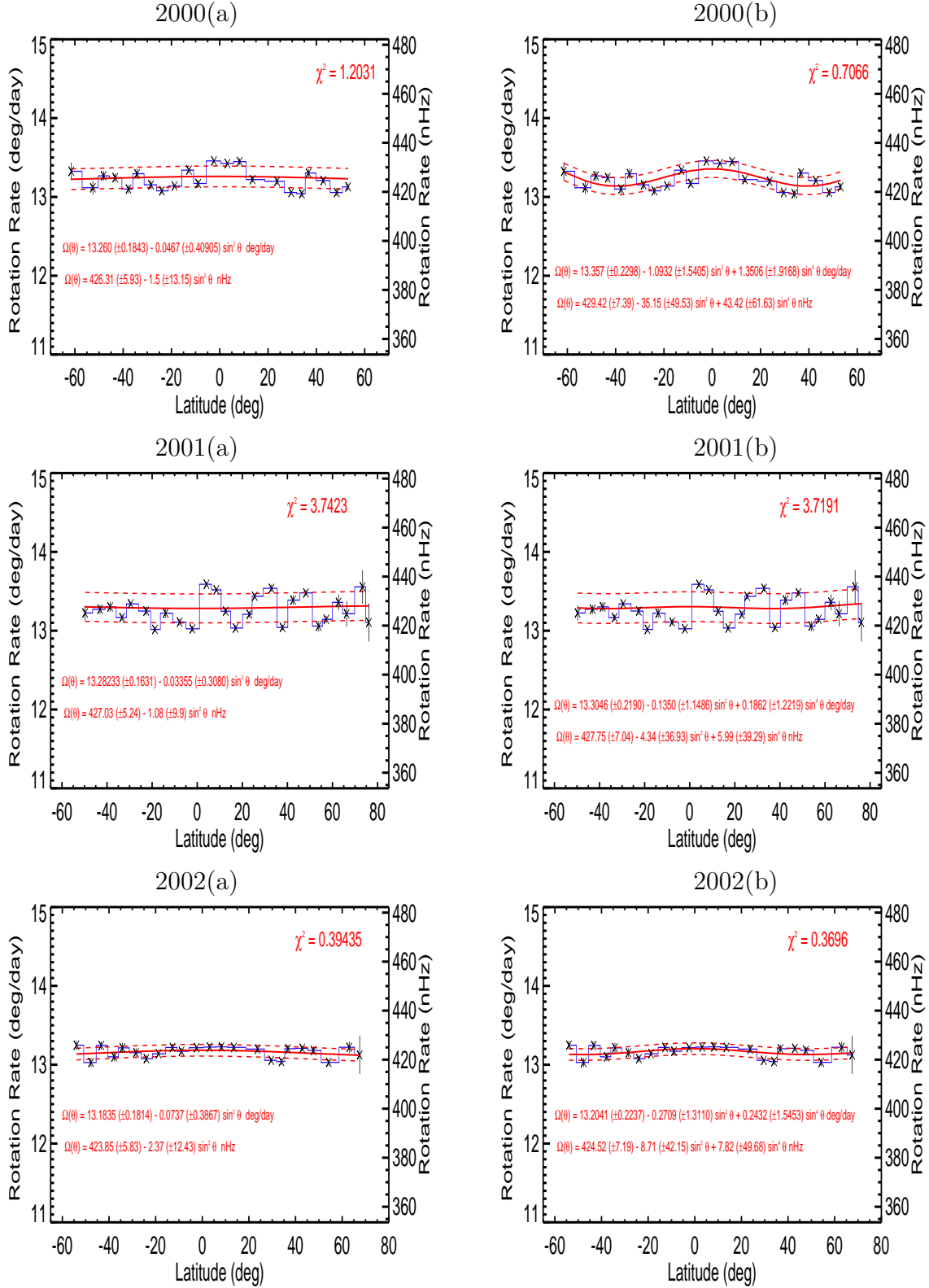


Figure 8: For the years 2000-2002, latitudinal variation of rotation rate of the coronal holes. Left panel is fitted with a law up to $\sin^2\theta$, whereas right panel is fitted with a law up to $\sin^4\theta$

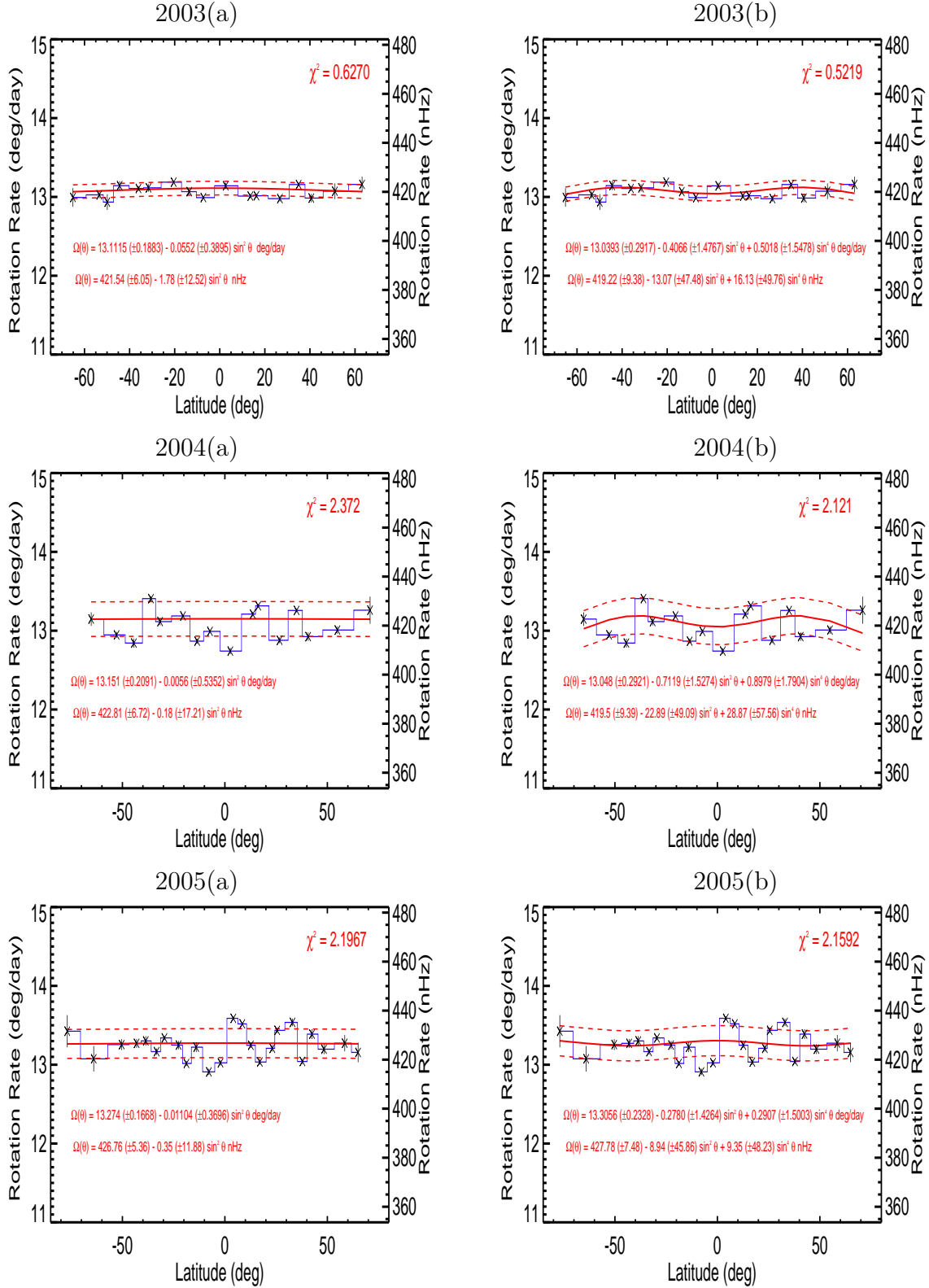


Figure 9: For the years 2003-2005, latitudinal variation of rotation rate of the coronal holes. Left panel is fitted with a law up to $\sin^2\theta$, whereas right panel is fitted with a law up to $\sin^4\theta$.

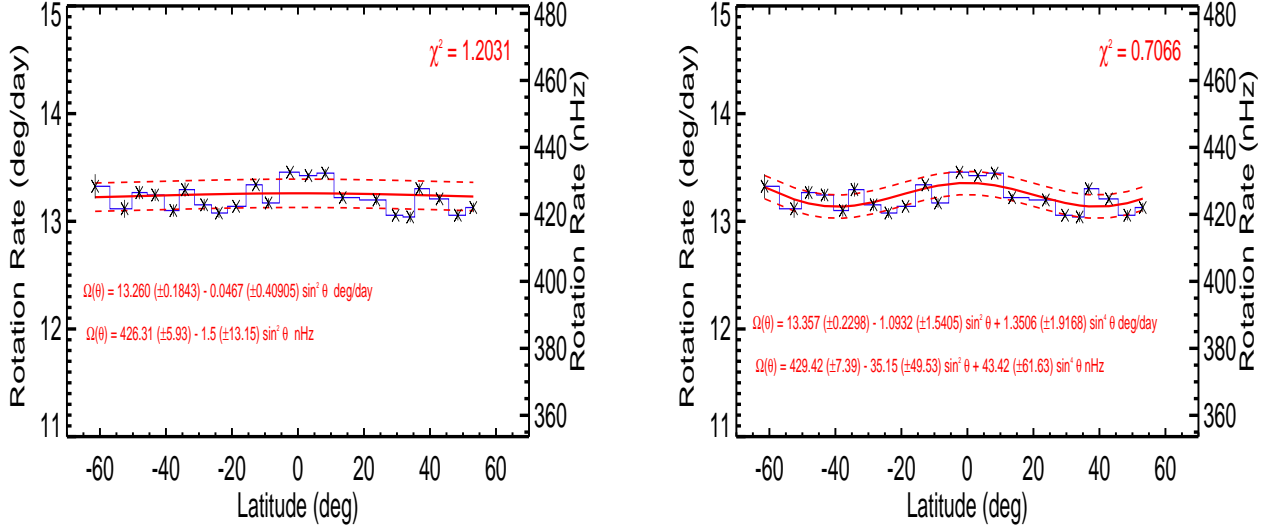


Figure 10: For the year 2006, latitudinal variation of rotation rate of the coronal holes. Left panel is fitted with a law up to $\sin^2\theta$, whereas right panel is fitted with a law up to $\sin^4\theta$.

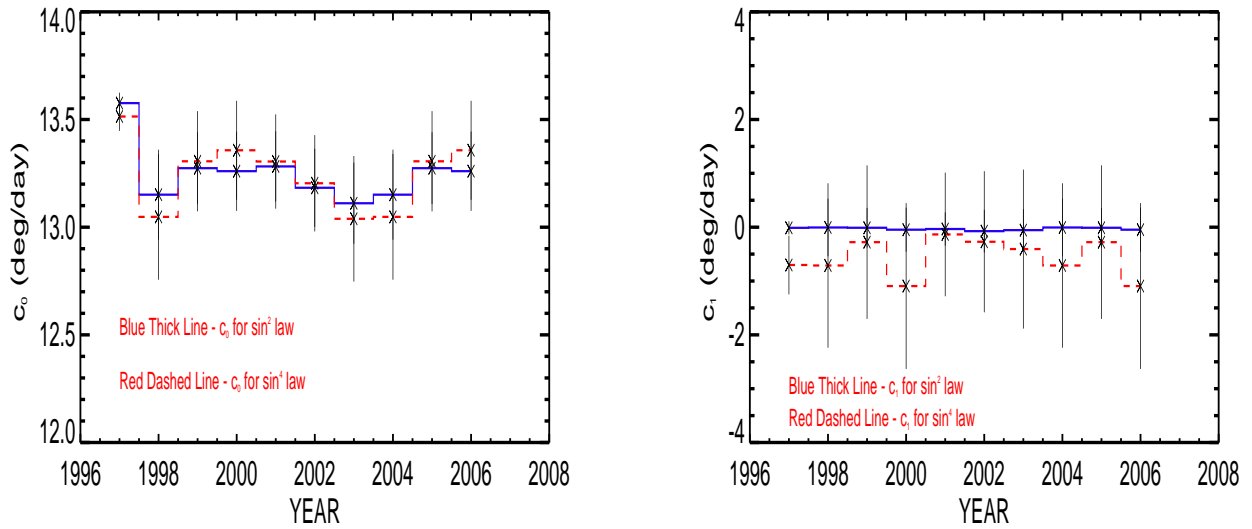


Figure 11: For the years, 1997-2006, variation of coefficients C_0 and C_1 that are obtained from the least square fit with a law up to $\sin^4\theta$.

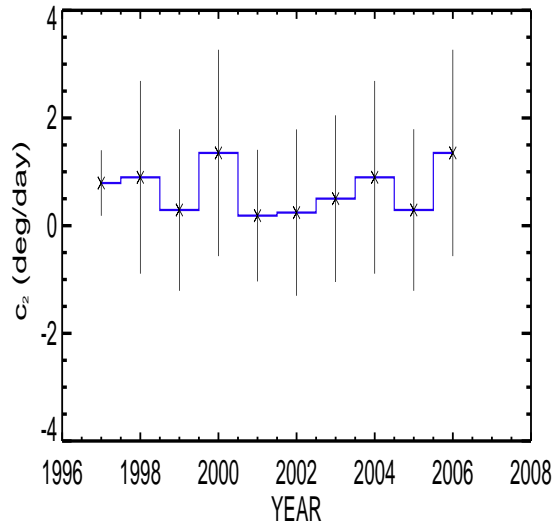


Figure 12: For the years, 1997-2006, variation of coefficients C_2 that is obtained from the least square fit with a law up to $\sin^4\theta$.

rotation rate of coronal holes are estimated to be $\sim 13.051 \pm 0.206$ deg/day for the equator, 12.993 ± 0.064 deg/day in the region of higher latitudes and, 12.999 ± 0.329 deg/day near the polar regions. Yearly variation of rotation rate of coronal holes is examined. For all the years 1997-2006, coronal holes rotate rigidly and magnitude of equatorial, high latitude and polar region rotation rates are independent of magnitude of solar activity.

Acknowledgments

This work has been carried out under “CAWSES India Phase-II program of Theme 1” sponsored by Indian Space Research Organization (ISRO), Government of India. SOHO is a mission of international cooperation between ESA and NASA.

REFERENCES

- Altschuler, M.D., Trotter, D.E., Orrall, F.Q.: 1972, Coronal Holes. *Solar Phys.* 26, 354.
- Antia, H. M., Basu, S & Chitre, S. M. 1998, *MNRAS*, 298, 543
- Antia, H. M. & Basu, S. 2010, *ApJ*, 720, 494
- Bagashvili, S. R.; Shergelashvili, B. M.; Japaridze, D. R.; Chargeishvili, B. B.; Kosovichev, A. G.; Kukhianidze, V.; Ramishvili, G.; Zaqarashvili, T. V.; Poedts, S.; Khodachenko, M. L.; De Causmaecker, P., 2017, *Astrophys Astron*, 603, 8
- Balthasar, H., Vazquez, M., & Woehl, H. 1986 *Astrophys Astron*, 155, 87
- Bohlin, J. D. 1977, *Solar Phys*, 51, 377
- Cranmer, S.R. 2009, *Living Reviews in Solar Phys*, 6, 3

- Dalgaard, C. J., & Schou, J. 1988, in "Seismology of the Sun and Sun-like stars", p.149
- Delaboudiniere, J. P. et al. 1995, *Solar Phys*, 162, 291
- Freeland, S.L., Handy, B.N.: 1998, *Solar Phys*. 182, 497
- Harvey, J. W., & Sheeley, N. R., Jr. 1979, *SSR*, 23, 139
- Harvey, J. W., & Sheeley, N. R., Jr. 1987, *Bulletin of the American Astronomical Society*, Vol. 19, p.935
- Hegde, M., Hiremath, K.M., Doddamani, V.H., Gurumath, S.R.: 2015, *Astrophysics and Astronomy* 36, 355.
- Hiremath, K. M 2002, *Astrophys Astron*, 386, 674
- Hiremath, K. M. 2009, *Sun and Geosphere*, 4, 16
- Hiremath, K. M. & Hegde, M.. 2013, *ApJ*, 763, 12
- Howard, R., & Harvey, J. 1970, *Solar Phys*, 12, 23
- Howard, R., Gilman, P. I., & Gilman, P. A. 1984, *ApJ*, 283, 373
- Howe, R. 2009, *Living Review in Solar Phys*, 6, 1
- Insley, J.E., Moore, V., & Harrison, R.A. 1995, *Solar Phys*, 160, 1
- Javaraiah, J. 2003, *Solar Phys*, 212, 23
- Japaridze, D. R.; Bagashvili, S. R.; Shergelasvili, B. M.; Chargeishvili, B. B., 2015, *Astrophys*, 58, 575
- Komm, R. W., Howard, R. F., & Harvey, J. W. 1993, *Solar Phys*, 145, 1
- Krieger, A.S., Timothy, A.F., & Roelof, E.C. 1973, *Solar Phys*. 29, 505
- Krista, L.D., Gallagher, P.T.: 2009, *Solar Phys*. 256, 87
- Madjarska, M. S., & Wiegmann, T. 2009, *Astrophys Astron*, 503, 991
- Navarro-Peralta, P., Sanchez-Ibarra, A.: 1994, *Solar Phys*. 153, 169
- Neupert, W.M., & Pizzo, V. 1974, *J. Geophys. Res.* 79, 3701
- Newton, H. W., & Nunn, M. L. 1951, *MNRAS*, 111, 413
- Nolte, J. T., Krieger, A. S., Timothy, A. F., Gold, R. E., Roelof, E. C., Vaiana, G., Lazarus, A. J., Sullivan, J. D., & McIntosh, P. S. 1976, 46, 303
- Oghrapishvili, N. B.; Bagashvili, S. R.; Maghradze, D. A.; Gachechiladze, T. Z.; Japaridze, D. R.; Shergelashvili, B. M.; Mdzinarishvili, T. G.; Chargeishvili, B. B., 2018, *Advances in Space Research*, 61, 3039
- Prabhu, K.; Ravindra, B.; Hegde, Manjunath; Doddamani, Vijayakumar H., 2018, *Astrophysics and Space Science*, 363, 11
- Obridko, V. N., & Shelting, B. D. 1989, *Solar Phys*, 124, 73
- Roša, D., Brajša, R., Vršnak, B., & Wöhl, H. 1995, *Solar Phys*, 159, 393
- Shelke, R. N., & Pande, M. C. 1985, *Solar Phys*, 95, 193
- Shugai, Yu. S., Veselovsky, I. S., & Trichtchenko, L. D. 2009, *Ge&Ae*, 49, 415

- Sivaraman, K.R., Gupta, S.S., Howard, R.F.: 1993, *Solar Phys.* 146, 27
- Skokić, I.; Brajša, R.; Roša, D.; Hržina, D.; Wöhl, H. 2014, *Solar Physics*, 289, 1471
- Snodgrass, H. B. 1983, *ApJ*, 270, 288
- Snodgrass, H. B., & Ulrich, R. K. 1990, *ApJ*, 351, 309
- Soon, W., Baliunas, S., Posmentier, E. S., & Okeke, P. 2000, *New Astronomy*, 4, 563
- Thompson, M. J. et al. 1996, *Science*, 272, 1300
- Temmer, M., Vršnak, B., Veronig, A.M.: 2007, *Solar Phys.* 241, 371
- Timothy, A.F., Krieger, A.S., Vaiana, G.S.: 1975, *Solar Phys.* 42, 135
- Thompson, M. J., Christensen-Dalsgaard, J., Jørgen, Miesch, Mark S. & Toomre, J. 2003, *AAPR*, 41, 599
- Ulrich, R. K., Boyden, J. E., Webster, L., & Shieber, T. 1988, in *ESA, Seismology of the Sun and Sun-Like Stars*, 286, 325
- Verbanac, G., Vršnak, B., Veronig, A., & Temmer, M. 2011, *Astron Astrophys*, 526, 20
- Wagner, W.J.: 1975, Solar rotation as marked by extreme-ultraviolet coronal holes. *Astrophys. J. Lett.* 198, L141. DOI. ADS.
- Wagner, W.J.: 1976, Rotational Characteristics of Coronal Holes. In: Bumba, V., Kleczek, J. (eds.) *Basic Mechanisms of Solar Activity*, IAU Symposium 71, 41.
- Wang, Y.M., *Space Sci Rev*, 2009, 144, 383
- Wilcox, J. M., & Howard, Robert 1970, *Solar Phys*, 13, 251
- Wittmann, A. D. 1996, *Solar Phys*, 168, 211
- Zirker, J. B. 1977, *Reviews of Geophysics and Space Physics*, 15, 257
- Zurbuchen, Th.; Bochslers, P.; von Steiger, R. 1996, in *Proceedings of the eighth international solar wind conference: Solar wind eight*. AIP Conference Proceedings, 382, p. 273